

# Terahertz absorption peak in graphene nanoplatelets/polylactic acid composites: effects of fine dispersion, agglomeration and percolation

D. Bychanok,<sup>1, a)</sup> P. Angelova,<sup>2</sup> A. Paddubskaya,<sup>1</sup> D. Meisak,<sup>1</sup> E. Shashkova,<sup>1</sup> M. Demidenko,<sup>1</sup> A. Plyushch,<sup>1</sup> E. Ivanov,<sup>2</sup> R. Krastev,<sup>2</sup> R. Kotsilkova,<sup>2</sup> F.Y. Ogrin,<sup>3</sup> and P. Kuzhir<sup>1,4</sup>

<sup>1)</sup> *Research Institute for Nuclear Problems Belarusian State University, 11 Bobruiskaya str., 220030, Minsk, Belarus*

<sup>2)</sup> *OLEM, Institute of Mechanics, Bulgarian Academy of Sciences, Sofia, Bulgaria*

<sup>3)</sup> *University of Exeter, Exeter, EX4 4QL, United Kingdom.*

<sup>4)</sup> *Tomsk State University, Tomsk 634050, Russian Federation*

(Dated: 5 August 2017)

The electromagnetic properties (EM) of composite materials based on polylactic acid (PLA) filled with graphene nanoplatelets (GNP) were investigated in the microwave (26-37 GHz) and terahertz (0.2-1 THz) frequency ranges. The maximum of imaginary part of dielectric permittivity was observed close to 0.6 THz for composites with 1.5 and 3 wt.% of GNP. The experimental data of complex dielectric permittivity of GNP/PLA composites was modelled using conventional Maxwell-Garnett theory. The effects of fine dispersion, agglomeration, and percolation in GNP-based composites on its electromagnetic constitutive parameters, presence and position of THz absorption peak are discussed on the basis of modeling results and experimental data. Along with evident interest to fabricated composites as the source for conductive filaments for 3D printing, GNP/PLA being below the percolation threshold, demonstrate the promising potential for effective absorption and manipulation of high frequency radiation.

Keywords: PLA composites, graphene nanoplatelets, terahertz absorption, electromagnetic radiation, Ka-band, Maxwell-Garnett theory

## I. INTRODUCTION

The progress in research of modern composites, as well as achievements of very promising mechanical and electromagnetic (EM) properties are often related to use of various types of nanostructural carbon fillers. Many researchers<sup>1-13</sup> showed that nanocarbon inclusions can significantly affect EM response of composites and provide an efficient way to tune their properties in wide frequency range.

Graphene nanoplatelets (GNP) are very perspective and economically feasible fillers for the production of conductive composites. Particularly, the recent investigations<sup>14-20</sup> of EM response of GNP/polymer composites in microwave and terahertz ranges showed their great potential for manipulation of EM radiation.

GNP is the high aspect ratio and high conductive material having a form of thin flakes of graphite. The typical diameter and thickness of GNP-particles provided by different manufacturer vary in the range  $D = 2 - 20 \mu\text{m}$ , and  $H = 4 - 20 \text{ nm}$ . The high aspect ratio, as well as high electrical conductivity of GNP particles generally define their EM properties in the microwave and THz ranges and make these carbon additives very promising for solving problems related to effective broadband absorption and shielding of EM radiation. In particular PLA filled with GNP, carbon nanotubes, and other nanocarbons is one of the best candidate to produced layered structures

or structures with different sophisticated geometries via additive manufacturing (see e.g.<sup>21-23</sup>)

The recent works showed<sup>18,20</sup> that EM properties of polymer composites based on GNP may be effectively described in microwave range using Maxwell-Garnett (M-G) theory for randomly dispersed conductive ellipsoids in the dielectric matrix. The local fields, as well as depolarization factors for ellipsoids may be easily calculated by analytical formulae<sup>24</sup>. In that case, the ellipsoid is a universal particle - it may be considered in the limited case as a sphere, needle, and disk, and widely used for prediction of EM properties of composites from statics and up to optical range<sup>25,26</sup>.

In the present communication, we will consider the polymer composites with GNP content below the percolation threshold and assume that GNP particles may be approximated as flattened conductive ellipsoids. This assumption is in good agreement with previous similar investigations in microwave range<sup>16,18,20</sup>. Moreover, the lateral dimensions, as well as the effective conductivity of GNP particles, make them especially interesting for terahertz frequency range. The results of simple modelling based on M-G theory presented below predicts the high absorption ability of such composites near 1 THz. The similar peak for carbon nanotubes composites was predicted and experimentally observed in<sup>27,28</sup>.

This paper is organized as follows: the second section describes details of modelling based on the Maxwell-Garnett theory. This formalism is then applied to explain the experimental data for the EM response of the GNP/PLA composites. The third section presents the fabrication of the composite materials and their experimental characterization. The experimental results re-

---

<sup>a)</sup> dzmitrybychanok@ya.ru; www.nano.bsu.by

lated to electromagnetic response of GNP/PLA composites in the microwave and terahertz ranges, comparison of the theoretical predictions and the experimental observation are presented in Section IV. The last Section of the manuscript is devoted to discussion of presented results together with effects of percolation and agglomeration in real composites. The conclusion part summarizes the general results most important to the further practical usage of the materials studied.

## II. MAXWELL-GARNETT MODELLING

Let us consider the mixture of conductive randomly oriented ellipsoidal particles in the dielectric matrix. In the case of low concentration of filler (below 10 %) the Maxwell-Garnett approach<sup>25</sup> is often applied to predict dielectric permittivity of such composite material. In classical form of M-G theory, the effective dielectric permittivity of a mixture is dependent on dielectric permittivity of inclusions. But usually nanocarbon fillers (carbon nanotubes, onion-like carbon, GNPs, carbon black and their agglomerates) are characterized in terms of polarizability  $\alpha$ <sup>27,28</sup> (here we use definition of polarizability as coefficient connecting electric field  $E$  and dipole moment of inclusion  $p = \alpha \varepsilon_0 E$ ,  $\varepsilon_0 = 8.85 \times 10^{12}$  F/m is vacuum permittivity, units for polarizability are [m<sup>3</sup>]). Through the paper M-G formulas are written in terms of inclusions polarizability and the effective dielectric permittivity of a composite is<sup>25</sup> (all equations below were written using SI units and assume an  $exp[i\omega t - ikz]$  harmonic time convention):

$$\varepsilon_{eff} = \varepsilon_m + \frac{\frac{1}{3} \sum_{i=a,b,c} n \alpha_i / V}{1 - \frac{1}{3} \sum_{i=a,b,c} \frac{N_i n \alpha_i / V}{\varepsilon_m}}, \quad (1)$$

where  $\varepsilon_m$  is the dielectric permittivity of matrix,  $n$  is the volume concentration of ellipsoids with semiaxes  $a, b, c$ ,  $\alpha_i$  is the polarizability of inclusions in  $i = a, b, c$  directions,  $N_i$  is the depolarization factor along  $i$ -axis,  $V$  is the volume of ellipsoid. The polarizability of conductive (i.e. with static conductivity  $\sigma$ ) ellipsoid surrounding by media with dielectric permittivity  $\varepsilon_m$  is<sup>25</sup>

$$\alpha_i(\nu, \sigma) = \frac{4\pi abc}{3} \frac{\varepsilon_m (1 - \frac{i\sigma}{2\pi\nu\varepsilon_0} - \varepsilon_m)}{\varepsilon_m + N_i (1 - \frac{i\sigma}{2\pi\nu\varepsilon_0} - \varepsilon_m)}, \quad (2)$$

where  $\nu$  is the frequency. The depolarization factors  $N_i$  for  $i = a, b, c$  directions may be calculated as<sup>24</sup>:

$$N_i = \frac{abc}{2} \int_0^\infty \frac{ds}{(s+i^2)\sqrt{(s+a^2)(s+b^2)(s+c^2)}}. \quad (3)$$

Important to note again, that presented above M-G equations are written in terms of polarizability of inclusions, which is more suitable for nanoscaled carbon filler.

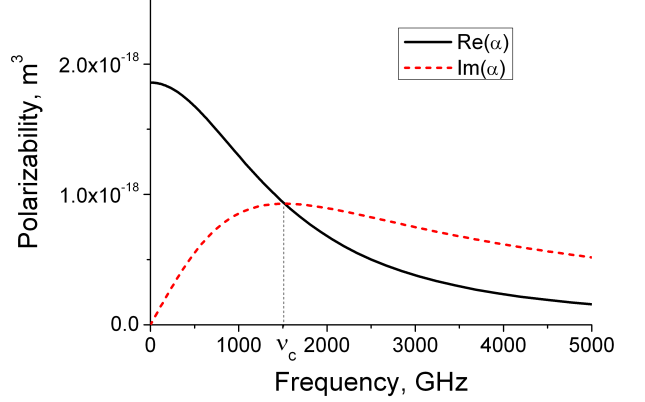


FIG. 1. Frequency dependence of polarizability  $\alpha_b = \alpha_c$  of flattened conductive ellipsoidal particle with diameter  $D=2b=2c=1.4 \mu\text{m}$ , thickness  $H=2a=17 \text{ nm}$  and conductivity  $\sigma=9000 \text{ S/m}$  in vacuum.

Nevertheless, the similar and equivalent M-G approach in terms of dielectric permittivity of inclusions was successfully applied for prediction and description of EM properties of GNP/epoxy composites in 8-18 GHz range<sup>18,20</sup>.

Due to strong dependence (see Eq.(2)) on depolarization factor, the polarizability of conductive inclusion is maximal in the direction parallel to the largest lateral dimension. Particularly, the frequency dependence of polarizability  $\alpha_b = \alpha_c$  of flattened conductive ellipsoidal particle with diameter  $D=2b=2c=1.4 \mu\text{m}$ , thickness  $H=2a=17 \text{ nm}$  and static conductivity  $\sigma=9000 \text{ S/m}$  in vacuum calculated using Eq.(2) is presented in Fig.1. The polarizability  $\alpha_a$  have significantly smaller values in comparison with  $\alpha_b$ , and their contribution at low frequencies (up to 5 THz) can be neglected. Below by default, we will consider and discuss the polarizability of inclusions along the largest lateral dimension.

Let us analyse Fig.1 together with Eq.(2). First of all, we see that in the static limit when  $\omega \rightarrow 0$  the polarizability is the real number. The value of Eq.(2) converges to classical values of static polarizability of conductive particle in the external electric field parallel to the largest lateral size of the particle. For example<sup>24</sup>, in case of sphere of radius  $R$  it is  $\alpha_s = 4\pi R^3$ , in case of disk of diameter  $D$  much larger than thickness  $H$   $\alpha_d = 2D^3/3$  and in case of needle of length  $L$  which is much larger than radius  $R$   $\alpha_n = 4\pi L^3/(24(\ln[2L/R] - 5/3))$ . Important to note that static polarizability is proportional to the largest lateral dimension raised to the third power and volume  $V$  of particle used in Eq.(1) is proportional to  $R^3$ ,  $D^3$  and  $L$  in the case of spheres, disks, and needles, correspondingly. Therefore, we clearly see that the high aspect ratio particles (disks and needles) much more significantly affect the EM properties of the composite in comparison with spheres with the same volume fraction.

Next, from examination of Fig.1 we see that the imaginary part of polarizability has a maximum at critical

frequency  $\nu_c$ . Above this frequency  $Im(\alpha)$ , related to Ohmic losses in conductive particles, starts to dominate. The trivial solve of equation  $\frac{\partial}{\partial \nu} Im(\alpha_i(\nu, \sigma)) = 0$  gives the simple expression for critical frequency

$$\nu_c = \frac{N_i \sigma}{2\pi \epsilon_0 (\epsilon_m - \epsilon_m N_i + N_i)}. \quad (4)$$

The  $Im(\alpha)$  maximum for conductive particles originates according to Eq.(1) the corresponding maximum of  $Im(\epsilon_{eff})$  in the composite. For example, for composite material based on the spherical graphite particles ( $\sigma = 120$  kS/m) in the dielectric matrix with  $\epsilon_m = 2.5$  the maximum of  $Im(\epsilon_{eff})$  is located in very high frequency range - near 360 THz. Nevertheless, from Eq.(4) it is clear that by playing with the conductivity of filler, their shape and aspect ratio it is possible to change smoothly the position of  $Im(\epsilon_{eff})$  maximum and shift them to much lower frequencies. Particularly, the flake structure of GNP as well as smaller value of conductivity ( $\sim 10$  kS/m<sup>18,20</sup>) allows to expect the absorption maximum near 1 THz (Fig.1).

Important to note that very often the experimental data of  $\epsilon$  for composites below percolation threshold may be satisfactorily fitted by Debye relaxation formula<sup>4,29</sup>:

$$\epsilon_D = \epsilon_\infty + \frac{\epsilon_s - \epsilon_\infty}{1 + i2\pi\nu\tau}, \quad (5)$$

where  $\tau$  is the relaxation time,  $\epsilon_s$  is the static permittivity, and  $\epsilon_\infty$  denotes the limiting high-frequency permittivity. The fitting parameters  $\tau, \epsilon_s, \epsilon_\infty$  are obtained from experiments. Important that the expressions for dielectric permittivity  $\epsilon_{eff}$  calculated using Eq.(1) and  $\epsilon_D$  calculated using Eq.(5) have after simplification the similar form and parameters of Debye model may be retrieved as  $\epsilon_s = \lim_{\nu \rightarrow 0} \epsilon_{eff}(\nu)$ ,  $\epsilon_\infty = \lim_{\nu \rightarrow \infty} \epsilon_{eff}(\nu)$ . The relaxation time  $\tau = 1/(2\pi\nu_c)$  is easy to calculate from critical frequency  $\nu_c$ .

Now let us apply Eqs.(1)-(2) for typical size and conductivity GNP fillers and check how they can modify the dielectric permittivity of the composite. From the electromagnetic point of view, the most important parameters are aspect ratio and conductivity of particles. The typical frequency dependence of dielectric permittivity of composite including 1.5 wt.% of particles with conductivity  $\sigma = 9000$  S/m and various aspect ratio (AR=diameter/thickness= $b/a$ ) is presented Fig.2.

From Fig.2(a) we can clearly see that AR of filler particles plays a crucial role in EM response of composite. The increase of AR leads to significant increase of both components of dielectric permittivity  $\epsilon = \epsilon' - i\epsilon''$ . For visualization of limits for  $\epsilon'$  and  $\epsilon''$  obtained within presented here modelling the same curves are displayed in Cole-Cole representation in the inset of Fig.2. Additionally, in accordance with the Eq.(4) absorption maximum shifts to the low-frequency region.

Typical frequency dependence of dielectric permittivity of composite including 1.5 wt.% of particles with

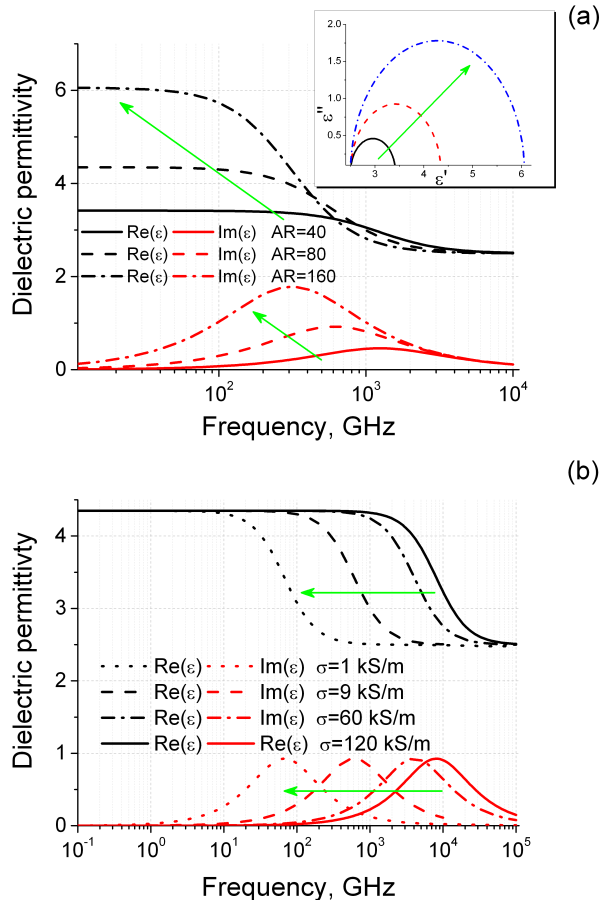


FIG. 2. (a) Frequency dependence of dielectric permittivity of composite including 1.5 wt.% of particles with conductivity  $\sigma = 9000$  S/m and various aspect ratio (the green arrow show the growth of AR from 40 to 160), (inset: the identical curves in the Cole-Cole representation) (b) The same for composite with AR=80 and various conductivity (the green arrow shows the decrease of  $\sigma$  from 120 to 1 kS/m).

AR=80 and various conductivity  $\sigma$  is presented in Fig.2(b). From this figure, we can clearly see that decrease of conductivity leads to decrease of position of the absorption peak. This is again the consequence of Eq.(4). Nevertheless, the change of  $\sigma$  leads to shifting of the peak but the shape of dielectric permittivity spectra remains the same. All curves from Fig.2(b) in Cole-Cole representation are equivalent (they are plotted in Fig.2(a) inset by red color).

All theoretical observations prove the possibility to observe terahertz absorption maximum in composites with well dispersed GNP particles inside the polymer matrix. These results are in good agreement with<sup>27,28,30</sup>. Application of presented formulae for composites with typical GNPs' parameters (aspect ratio, size, conductivity, etc.) shows that these samples are good for terahertz absorption due to presence of  $\epsilon''$  maximum near 1 THz.

### III. COMPOSITES FABRICATION AND CHARACTERIZATION

In the present communication, we used polymer matrix suitable for further 3D printing applications. Particularly, the poly(lactic) acid polymer (PLA) Ingeo 750 1D from Nature Works, USA was used as matrix polymer for the preparation of composite materials samples. GNPs produced from Times Nano, China were used as filler for the preparation of nanocomposites<sup>31</sup>. The source GNP-particles have a thickness in range 4-20 nm and diameter in range 5-10  $\mu\text{m}$ .

The samples were prepared using the following procedure. The PLA 750 1D was dissolved in chloroform in ratio 1:3. Suspensions of GNP and were prepared in 200 ml chloroform by ultrasonic mixing and added to the dissolved PLA. The final mixture was mechanically stirred for 60 min and dried in a vacuum oven for 24 hours at 70°C. Compositions with  $\eta = 0\%$ , 1.5% and 3% wt. of GNP in PLA in form of 1 mm thick plane parallel plate were prepared by this solution blending technique.

The transmission electron microscopy (TEM) analysis of GNP/PLA composites was made by TEM JEOL JEM 2100 in bright field (BF) mode at accelerating voltage 200 kV. Results of TEM-analysis showing that the composite consists of separated GNP particles in the PLA matrix. The typical TEM-image of obtained composites is presented in Fig.3(a)-(b). The particles have a complex multilayer-graphene-based structure reminiscent of crumpled paper. The typical lateral size of GNP inclusion is 1-2  $\mu\text{m}$  (Fig.3(a)) and the thickness of multilayer-graphene forming the GNP is varies in range 4-20 nm (Fig.3(b)) in good correspondence with the manufacturer data sheet<sup>31</sup>. Due to breaking during high power sonication treatment the average diameter of particles was decreased to several microns.

The typical Raman spectra of GNP/PLA composites is shown in Fig.4. The peaks observed at 1363, 1576 and 2743  $\text{cm}^{-1}$  are originated from GNP, 871 and 2996  $\text{cm}^{-1}$  are contributed by PLA matrix. The largest 2G 1576  $\text{cm}^{-1}$  peak is typical for high ordered graphite.

The electromagnetic response of a GNP/PLA composites was experimentally investigated in the Ka-band (26 - 37 GHz) using a scalar network analyser ELMIKA R2-408R. All measurements were carried out in a  $7.2 \times 3.4$  mm waveguide system described in details our recent work<sup>10</sup>. The dielectric permittivity  $\epsilon$  was then calculated based on methodology<sup>32</sup>.

THz measurements were carried out using a commercial THz time-domain spectrometer "T-Spec" by EK-SPLA. A  $1050 \pm 40$  nm wave length pumping laser having 50-150 fs pulse duration and more than 40 mW output power at approximately 80 MHz pulse repetition rate was used to excite a photoconductor antenna and produced THz radiation up to 2 THz. The spectrometer, THz emitter, and detector consist of a microstrip antenna integrated with a photoconductor (low temperature grown GaBiAs) and silicon lens. The sample in the form of

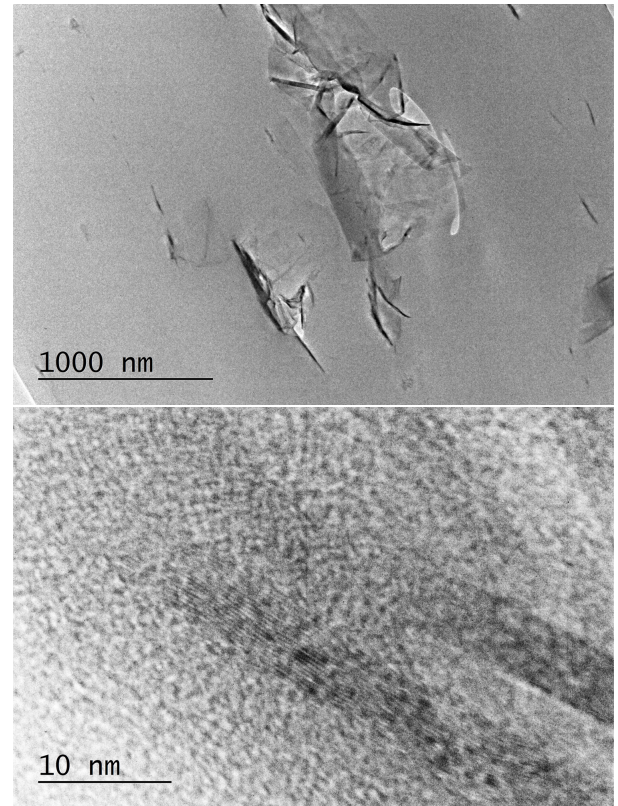


FIG. 3. TEM-image of (a) the whole GNP-particle in the composite (b) area of GNP-particle oriented perpendicular to the electron beam.

a plane parallel plate was placed between emitter and detector normally to the initial EM wave. The THz detector output is proportional to the instant electrical field strength of the THz pulse during the ultra short pumping pulse. The Fourier transform of the waveform of electrical field of THz radiation gives the frequency dependence of complex transmission coefficient of investigated sample used for  $\epsilon$  calculations.

### IV. EXPERIMENTAL RESULTS

The results of calculation of dielectric permittivity from the experimentally measured data in the microwave and THz ranges are presented in Fig.5 with scatters.

First of all the maximum of  $\epsilon''$  is clearly seen near  $\nu_c = 0.6$  THz in Fig.5. The absolute value of  $\epsilon''$  is increasing with GNP content. The real part of dielectric permittivity has a pronounced bend near 0.6 THz.

The best fit of experimental data using Eqs.(1)-(2) is presented in Fig.5 with lines. The following parameters of particles were used: electrical conductivity  $\sigma=9000$  S/m, GNP thickness  $H=2a=17$  nm, GNP diameter  $D=2b=2c=1.4$   $\mu\text{m}$ . These parameters are in good correspondence with datasheets provided by GNP manufacturer<sup>31</sup> and also with other GNP-related

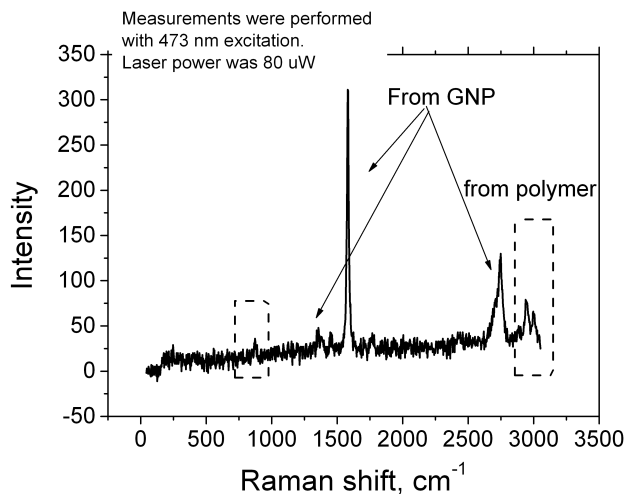


FIG. 4. Raman spectra of GNP/PLA composites (arrows show GNP contribution, peaks in dedicated area originated by PLA).

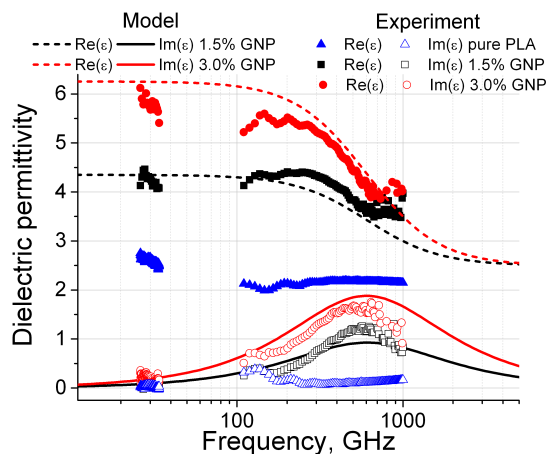


FIG. 5. Frequency dependence of dielectric permittivity  $\epsilon$  obtained from experiment (scatters) and using modelling (lines).

publications<sup>15–18,20</sup>. Dielectric permittivity of PLA matrix was used  $\epsilon_m = 2.5$ . The volume fraction of GNP was obtained from mass fraction  $\eta$  as  $n = (1 + \frac{1-\eta}{\eta} \frac{\rho_{GNP}}{\rho_{PLA}})^{-1}$ , where  $\rho_{PLA} = 1430 \text{ kg/m}^3$ ,  $\rho_{GNP} = 2100 \text{ kg/m}^3$  are density of PLA-matrix and GNP, correspondingly.

Results of modelling are in good agreement with experimental data. In the next section, we will discuss the general features of GNP based composites together with overview and outlook for possible practical use.

## V. DISCUSSION

As we mentioned above, the composites with GNP content below the percolation threshold were investigated. To observe THz absorption maximum composite should be prepared with very high level of GNP distribution

homogeneity, i.e. particles should be isolated from each other. It is very difficult to realize in practice due to problems with agglomeration of carbon particles<sup>33,34</sup>. Additionally, at higher concentrations, the percolation occurs. The next subsection will discuss the influence of these effects on the appearance and position of the THz absorption peak.

### A. Effect of agglomerates

Agglomerates and connected particles may be considered as structures with higher aspect ratio and lower effective conductivity. The effective conductivity decreases due to the presence of contacts between particles. The agglomerates and connected particles form a percolation network with complex structured conductive regions. They may be considered as prolonged particles<sup>18</sup> with increased effective AR. According to Eq.(4) both of these parameters leads to significant decrease of  $\nu_c$ . To demonstrate effect of agglomerates we consider mixture of 1.5 wt.% of mentioned above GNP particles and 0.15% of agglomerates with diameter  $D = 2b = 2c$ , macroscopic length  $L=0.2 \text{ mm}$  and conductivity  $\sigma=3000 \text{ S/m}$ . In this case of the multiphase mixture, the sums in Eq.(1) should include terms for all fractions in the composite. The dielectric permittivity spectra for one- and two-component of agglomerates/GNP/PLA composite are presented in Fig.6(a). One can see that at low frequencies the contribution of agglomerates is dominated and in the range 5-50 GHz (see the grey region in Fig6(a)) both components are decreasing with frequency as it was observed, e.g. in<sup>16,18,20</sup>.

In the Cole-Cole representation (Fig.6(b)) spectra have a form of two engaged hemispheres. When the content of the filler increases, a number of agglomerates also increases. In this situation, the large hemisphere merged the smaller in Fig.6(b) and THz peak is spread and became invisible. Moreover, the contribution of agglomerated or percolated particles will be excluded from high-frequency absorption peak and should be taken into account at low-frequency absorption. In this case, the frequency spectra of  $\epsilon$  will be dominated by the contribution of agglomerates and the high-frequency THz-peak will be significantly dumped. That is why it is very important to prepare well dispersed GNP composites to observe high-frequency THz absorption phenomena. This situation was widely discussed in<sup>18,20</sup>, where authors used a mixture of oblate and prolate ellipsoids to explain the EM properties of similar GNP/epoxy composites at lower frequencies (8-18 GHz). Actually, from the present analysis, we can clearly see that well dispersed GNP/PLA composite may be used as selective THz absorber transparent for microwave radiation.

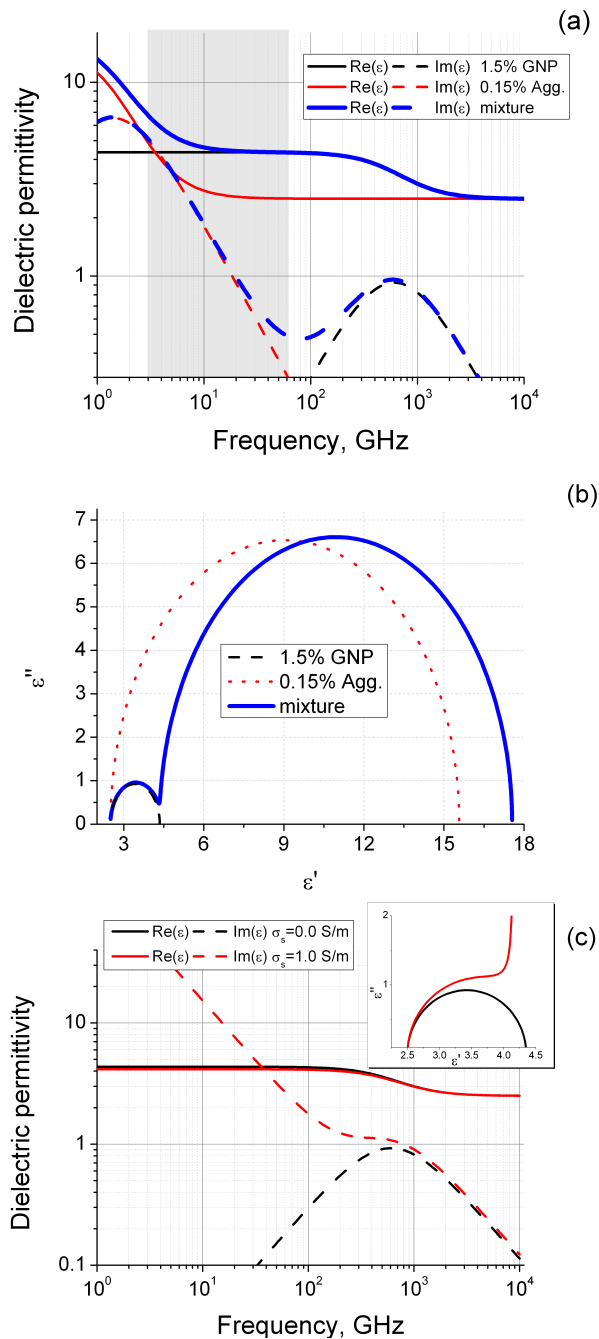


FIG. 6. (a) Frequency dependence of dielectric permittivity  $\epsilon$  of composites containing 1.5 % GNP, 0.15% agglomerates, and their mixture (b) the identical curves in the Cole-Cole representation, (c) the same as (a) for 1.5 % GNP inside the matrix with and without DC conductivity  $\sigma_s$ .

## B. Effect of percolation

When the concentration of filler reaches the percolation threshold agglomerates or arrays of connected particles starts to be comparable to the lateral dimension of whole sample and material starts to be conductive

in DC. The description of EM processes in agglomerates is a complex problem which may be solved within percolation theory and through applying time-consuming Monte-Carlo modelling<sup>35</sup>.

Nevertheless, to understand the general features of broadband dielectric permittivity spectra of percolated composites it is possible to assume that dielectric permittivity of the matrix in percolated composites starts to be complex  $\epsilon_m^* = \epsilon_m - i\sigma_s / (2\pi\nu\epsilon_0)$  where  $\sigma_s$  is the static conductivity of the composite. In this case,  $Im(\epsilon_{eff})$  has singularity at  $\nu \rightarrow 0$ . The comparison of corresponded spectra of composite consisting of 1.5% of mentioned above GNP particles inside the neat PLA matrix and inside the matrix with dielectric permittivity  $\epsilon_m^*$  and  $\sigma_s = 1$  S/m is presented in Fig.6(c). We see from this figure that percolation generally affects the  $Im$  part of the dielectric permittivity, whereas the real part is influenced very slightly, decreasing at low frequencies due to shunting of conductive particles by conducting matrix. The THz absorption maximum may be potentially observed in percolative composites, for small values of conductivity  $\sigma_s$ . Let us examine spectra from Fig.6(c) in the Cole-Cole representation (see inset of Fig.6(c)). The position of singularity is very important for the possibility of experimental THz peak observation. If  $\sigma_s$  is less than  $\sim 1$  S/m the singularity is moving to the right from the red curve and THz peak starts to be more pronounced. If  $\sigma_s$  is increases than singularity shifts to the left the terahertz absorption peak in that case disappears.

Summarizing we can conclude that in the case of real percolative composite including arrays of connected particles forming the percolation paths, agglomerates and isolated particles the contribution of agglomerates plays dominate role in formation of  $Re(\epsilon)$  at lower frequencies, particles included to conductive paths are responsible mainly for  $Im(\epsilon)$  and isolated particles are form THz absorption peak.

## VI. CONCLUSIONS

The possibility of experimental observation of maximum of terahertz absorption in GNP/PLA composites was demonstrated and discussed on the basis of Maxwell-Garnett modelling. The simple relations between position of absorption maximum and geometrical and conductive parameters of inclusions are derived. An absorption maximum was experimentally observed near frequency 0.6 THz for the GNP/PLA composites with 1.5 and 3 wt.% of graphene fillers, which is below the percolation threshold. The experimental data were fitted using Maxwell-Garnett formulae. Effects of percolation and agglomeration are discussed in view of responsibility for electromagnetics constitutive parameters of the GNP comprising composites and position, if any, of THz absorption peak.

## VII. ACKNOWLEDGEMENTS

The work is supported by H2020 RISE 734164 Graphene 3D, U.S. Air Force through CRDF Global Agreement grant AF20-15-61804-1 and EU FP7-PEOPLE-2013-IRSES project FP7-612285 CANTOR, PK is thankful for support by Tomsk State University Competitiveness Improvement Program. Authors are grateful to Prof. Daniela Karashanova, Institute of Optical Materials and Technologies Bulgarian Academy of Sciences for TEM measurements.

## VIII. REFERENCES

- <sup>1</sup>F. Qin and C. Brosseau, "A review and analysis of microwave absorption in polymer composites filled with carbonaceous particles," *J. Appl. Phys.* **111**, 061301–24 (2012).
- <sup>2</sup>C. Brosseau, P. Molinie, F. Boulic, and F. Carmona, "Mesostructure, electron paramagnetic resonance, and magnetic properties of polymer carbon black composites," *J. Appl. Phys.* **89**, 8297–8310 (2001).
- <sup>3</sup>P. Kuzhir, A. Paddubskaya, D. Bychanok, A. Nemilentsau, M. Shuba, A. Plusch, S. Maksimenko, S. Bellucci, L. Coderoni, F. Micciulla, I. Sacco, G. Rinaldi, J. Macutkevic, D. Seliuta, G. Valusis, and J. Banys, "Microwave probing of nanocarbon based epoxy resin composite films: Toward electromagnetic shielding," *Carbon- or Nitrogen-Containing Nanostructured Composite Films*, *Thin Solid Films* **519**, 4114–4118 (2011).
- <sup>4</sup>D. Bychanok, P. Kuzhir, S. Maksimenko, S. Bellucci, and C. Brosseau, "Characterizing epoxy composites filled with carbonaceous nanoparticles from dc to microwave," *J. Appl. Phys.* **113**, 124103–6 (2013).
- <sup>5</sup>O. Sedelnikova, M. Kanygin, E. Korovin, L. Bulusheva, V. Suslyayev, and A. Okotrub, "Effect of fabrication method on the structure and electromagnetic response of carbon nanotube/polystyrene composites in low-frequency and ka bands," *Composites Science and Technology* **102**, 59–64 (2014).
- <sup>6</sup>G. Gradoni, D. Micheli, V. Mariani Primiani, F. Moglie, and M. Marchetti, "Determination of the electrical conductivity of carbon/carbon at high microwave frequencies," *Carbon* **54**, 76–85 (2013).
- <sup>7</sup>V. I. Suslyayev, V. L. Kuznetsov, V. A. Zhuravlev, I. N. Mazov, E. Y. Korovin, S. I. Moseenkov, and K. V. Dorozhkin, "An investigation of electromagnetic response of composite polymer materials containing carbon nanostructures within the range of frequencies 10 mhz 1.1 thz," *Russian Physics Journal* **55**, 970–976 (2013).
- <sup>8</sup>B. De Vivo, P. Lamberti, V. Tucci, L. Guadagno, L. Vertuccio, V. Vittoria, and A. Sorrentino, "Comparison of the physical properties of epoxybased composites filled with different types of carbon nanotubes for aeronautic applications," *Advances in Polymer Technology* **31**, 205–218 (2012).
- <sup>9</sup>A. Yu, P. Ramesh, M. E. Itkis, E. Bekyarova, and R. C. Haddon, "Graphite nanoplatelet/epoxy composite thermal interface materials," *The Journal of Physical Chemistry C*, *J. Phys. Chem. C* **111**, 7565–7569 (2007).
- <sup>10</sup>D. Bychanok, G. Gorokhov, D. Meisak, A. Plyushch, P. Kuzhir, A. Sokal, K. Lapko, A. Sanchez-Sanchez, V. Fierro, A. Celzard, C. Gallagher, A. P. Hibbins, F. Y. Ogrin, and C. Brosseau, "Exploring carbon nanotubes/batio3/fe3o4 nanocomposites as microwave absorbers," *Progress In Electromagnetics Research C* **66**, 77–85 (2016).
- <sup>11</sup>P. Kuzhir, A. Paddubskaya, A. Plyushch, N. Volynets, S. Maksimenko, J. Macutkevic, I. Kranauskaite, J. Banys, E. Ivanov, R. Kotsilkova, A. Celzard, V. Fierro, J. Zicans, T. Ivanova, R. Merijs Meri, I. Bochkov, A. Cataldo, F. Micciulla, S. Bellucci, and P. Lambin, "Epoxy composites filled with high surface area-carbon fillers: Optimization of electromagnetic shielding, electrical, mechanical, and thermal properties," *Journal of Applied Physics*, *Journal of Applied Physics* **114**, 164304– (2013).
- <sup>12</sup>I. Kranauskaite, J. Macutkevic, P. Kuzhir, N. Volynets, A. Paddubskaya, D. Bychanok, S. Maksimenko, J. Banys, R. Juskenas, S. Bistarelli, A. Cataldo, F. Micciulla, S. Bellucci, V. Fierro, and A. Celzard, "Dielectric properties of graphite-based epoxy composites," *Phys. Status Solidi A* **211**, 1623–1633 (2014).
- <sup>13</sup>A. Plyushch, J. Macutkevic, P. P. Kuzhir, J. Banys, V. Fierro, and A. Celzard, "Dielectric properties and electrical conductivity of flat micronic graphite/polyurethane composites," *Journal of Nanophotonics* **10**, 012511–012511 (2015).
- <sup>14</sup>J. Li, J.-K. Kim, and M. L. Sham, "Conductive graphite nanoplatelet/epoxy nanocomposites: effects of exfoliation and uv/ozone treatment of graphite," *Scripta Materialia* **53**, 235–240 (2005).
- <sup>15</sup>M.-T. Hung, O. Choi, Y. S. Ju, and H. Hahn, "Heat conduction in graphite-nanoplatelet-reinforced polymer nanocomposites," *Applied Physics Letters* **89**, 023117– (2006).
- <sup>16</sup>S.-E. Lee, O. Choi, and H. T. Hahn, "Microwave properties of graphite nanoplatelet/epoxy composites," *Journal of Applied Physics*, *Journal of Applied Physics* **104**, 033705– (2008).
- <sup>17</sup>H. L. Liu, G. Carr, K. Worsley, M. Itkis, R. Haddon, A. Caruso, L. Tung, and Y. Wang, "Exploring the charge dynamics in graphite nanoplatelets by thz and infrared spectroscopy," *New Journal of Physics* **12**, 113012– (2010).
- <sup>18</sup>M. S. Sarto, A. G. D'Aloia, A. Tamburrano, and G. De Bellis, "Synthesis, modeling, and experimental characterization of graphite nanoplatelet-based composites for emc applications," *IEEE Transactions on Electromagnetic Compatibility* **54**, 17–27 (2012).
- <sup>19</sup>A. Plyushch, J. Macutkevic, P. Kuzhir, J. Banys, D. Bychanok, P. Lambin, S. Bistarelli, A. Cataldo, F. Micciulla, and S. Bellucci, "Electromagnetic properties of graphene nanoplatelets/epoxy composites," *Composites Science and Technology* **128**, 75–83 (2016).
- <sup>20</sup>F. Marra, A. G. DAloia, A. Tamburrano, I. M. Ochando, G. De Bellis, G. Ellis, and M. S. Sarto, "Electromagnetic and dynamic mechanical properties of epoxy and vinylester-based composites filled with graphene nanoplatelets," *Polymers* **8**, 272 (2016).
- <sup>21</sup>"3d black magic filament. <http://www.blackmagic3d.com/conductive-graphene-3d-printing-pla-filament-p/grphn-175.htm>,".
- <sup>22</sup>A. Paddubskaya, N. Valynets, P. Kuzhir, K. Batrakov, S. Maksimenko, R. Kotsilkova, H. Velichkova, I. Petrova, I. Bir, K. Kertesz, G. I. Mrk, Z. E. Horvth, and L. P. Bir, "Electromagnetic and thermal properties of three-dimensional printed multilayered nano-carbon/poly(lactic) acid structures," *Journal of Applied Physics*, *Journal of Applied Physics* **119**, 135102– (2016).
- <sup>23</sup>R. Kotsilkova, E. Ivanov, P. Todorov, I. Petrova, N. Volynets, A. Paddubskaya, P. Kuzhir, V. Uglov, I. Biro, K. Kertesz, G. I. Mark, and L. P. Biro, "Mechanical and electromagnetic properties of 3d printed hot pressed nanocarbon/poly(lactic) acid thin films," *Journal of Applied Physics*, *Journal of Applied Physics* **121**, 064105– (2017).
- <sup>24</sup>L. D. Landau and E. Lifshitz, *Course of Theoretical Physics. Vol. 8: Electrodynamics of Continuous Media* (Oxford, 1960) pp. –.
- <sup>25</sup>A. Priou, *Dielectric properties of heterogeneous materials*, Vol. 6 (Elsevier Science Ltd, 1992) pp. –.
- <sup>26</sup>C. F. Bohren and D. R. Huffman, *Absorption and scattering of light by small particles* (John Wiley & Sons, 2008) pp. –.
- <sup>27</sup>M. V. Shuba, A. V. Melnikov, A. G. Paddubskaya, P. P. Kuzhir, S. A. Maksimenko, and C. Thomsen, "Role of finite-size effects in the microwave and subterahertz electromagnetic response of a multiwall carbon-nanotube-based composite: Theory and interpretation of experiments," *Phys. Rev. B* **88**, 045436– (2013).

- <sup>28</sup>G. Y. Slepyan, M. V. Shuba, S. A. Maksimenko, C. Thomsen, and A. Lakhtakia, "Terahertz conductivity peak in composite materials containing carbon nanotubes: Theory and interpretation of experiment," *Phys. Rev. B* **81**, 205423– (2010).
- <sup>29</sup>A. K. Jonscher, "Dielectric relaxation in solids," *Journal of Physics D: Applied Physics* **32**, R57– (1999).
- <sup>30</sup>L. Ju, B. Geng, J. Horng, C. Girit, M. Martin, Z. Hao, H. A. Bechtel, X. Liang, A. Zettl, Y. R. Shen, and F. Wang, "Graphene plasmonics for tunable terahertz metamaterials," *Nat Nano* **6**, 630–634 (2011).
- <sup>31</sup><http://www.timesnano.com/en/view.php?prt=3,36,65,104>,".
- <sup>32</sup>"Standard test method for measuring relative complex permittivity and relative magnetic permeability of solid materials at microwave frequencies, astm d5568-08, 2009.".
- <sup>33</sup>M. Shuba, A. Paddubskaya, P. Kuzhir, S. Maksimenko, V. Ksenevich, G. Niaura, D. Seliuta, I. Kasalynas, and G. Valusis, "Soft cutting of single-wall carbon nanotubes by low temperature ultrasonication in a mixture of sulfuric and nitric acids," *Nanotechnology* **23**, 495714– (2012).
- <sup>34</sup>M. Shuba, S. Maksimenko, and A. Lakhtakia, "Electromagnetic wave propagation in an almost circular bundle of closely packed metallic carbon nanotubes," *Physical Review B* **76**, 155407– (2007).
- <sup>35</sup>G. Spinelli, A. Giustiniani, P. Lamberti, V. Tucci, and W. Zamboni, "Numerical study of electrical behaviour in carbon nanotube composites," *International Journal of Applied Electromagnetics and Mechanics* **39**, 21–27 (2012).